10th ANKARA INTERNATIONAL AEROSPACE CONFERENCE **AIAC-2019-136**
18-20 September 2019 - METU, Ankara TURKEY

PREDICTION OF WIND TUNNEL WALL EFFECTS USING PANEL METHODS

Yusuf Demiroglu[1]
Istanbul Technical University
Istanbul, Turkey

M. Adil Yukselen[2]
Istanbul Technical University
Istanbul, Turkey

ABSTRACT

Presence of the wind tunnel test section walls create a change in the flow field around a lifting or non-lifting body in a wind tunnel, relative to the free flow state. Prediction of this effect is essential in terms of experimental aerodynamics. In this study, two computer program were developed to calculate 2- and 3- dimensional incompressible potential flows in free flow or in wind tunnel test section to evaluate wind tunnel wall effects. In the 2D case, source and vortex distributions are used for the airfoils and source distributions for the walls with a Neumann type surface boundary condition. In the 3D case Vortex Ring method is used for lifting surfaces and source panel method for non-lifting bodies. For the wind tunnel walls the 3D computer program has a choice between the Vortex Ring method and 3D source method. Several test applications of the programs are given.

INTRODUCTION

Wind tunnels have been used for over a century in the world aviation industry and research centers to be able to obtain aerodynamic characteristics of air vehicles and their wings, fuselages, and other components experimentally. One of the most important problems in wind tunnel experiments is the wall effects and their correction.

In order to meet the Reynolds number requirements, it is often desirable that a wind tunnel test section be as wide as possible. However, since the large test room will create high investment and operating costs, the wind tunnel test rooms must always be of limited size. In this case, it is necessary to perform the experiments in this limited test section with the largest size models. On the other hand, the presence of wind tunnel walls around a test model causes a change in the flow field. As a result, the measured aerodynamic characteristics of the model differ from its expected characteristics in isolated case. This difference is considered as a wind tunnel wall effect. The larger the ratio between the sizes of model and the test section, the larger the wall effect. But, if this ratio is reduced, The Reynolds number requirement will be less covered. Therefore, it is necessary to find an optimal solution between these two issues. In this regard, determining and correcting wall effects is one of the important issues of experimental aerodynamics.

[1] BSc in Astronautical Engineering Department, Email: demirogluy@itu.edu.tr
[2] Prof. in Aeronautical Engineering Department , Email: yukselen@itu.edu.tr

From the beginning of wind tunnel use, various methods have been developed for estimating and correcting wall effects. Most of these methods, analytical and semi-empirical, based on the circulation, have been extensively described by [Garner, 1967], [Mokry and Chan, 1983] and [Allmaras, 1986]. With the development of computers, it has become possible to use various computational aerodynamic techniques for more accurate estimation and correction of wall effects. Although CFD techniques are the highest-level methods for the calculation of viscous flow fields at present, since such methods require high computer speed and capacity, panel methods can be preferred as a lower-level alternative to calculate wall effects. [Katz and Plotkin, 2001]. In the panel methods the flow field is assumed as potential. At small and moderate angles of attack, the viscous effects on the aerodynamic coefficients of the wings and other thin lifting surfaces are small, especially in terms of predicting wall effects [Browne, Katz, 1990]. However, it is necessary to be careful for viscous effects at high angles of attack. Although wind tunnel experiments and the wall effects in this context are very important for the aviation industry, it is noteworthy that these issues have not come to the forefront in our country. Therefore, in this paper, a panel-method based study is performed to estimate the wind tunnel wall effects on two- and three-dimensional lifting and non-lifting surfaces. For the two dimensional case, Hess-Smith Panel Method [Hess and Smith, 1967] is used. For the three dimensional case, Vortex Ring Method (VRM) [Katz and Plotkin, 2001] is preferred for lifting surface and source panel method of Hess and Smith [Hess and Smith, 1967] for non-lifting surfaces. In 3D case the wind tunnel walls can be modelled by VRM or source panels. Two computer programs are developed for 2- and 3-D cases, following the formulations given by Yukselen [Yukselen, 2015, 2017] for multi-element wings and bodies. Figure 1 shows the image of an aircraft modeled by these methods in a wind tunnel test section.

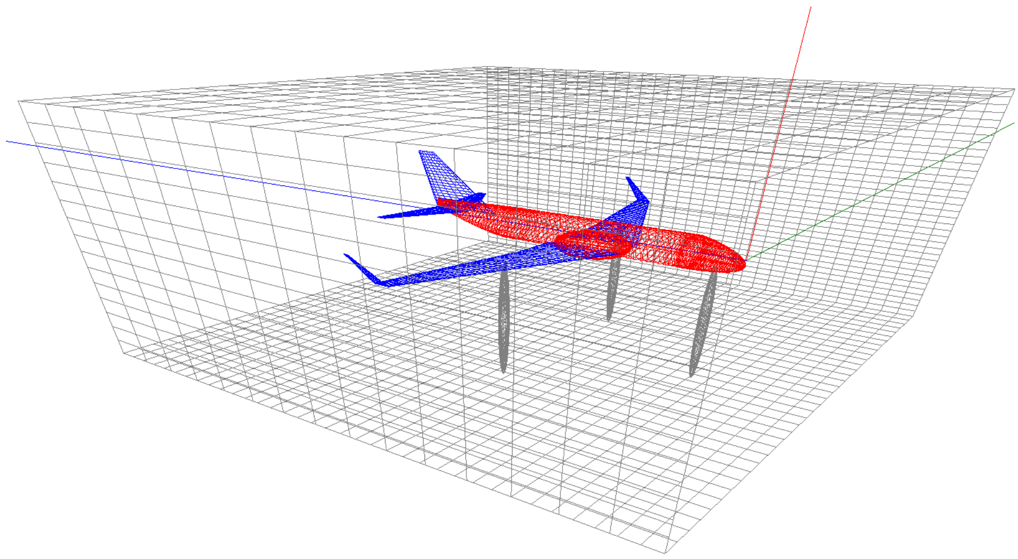

Figure 1: Image of an aircraft example placed in a wind tunnel test section from GUI of the program

METHOD

In this study low-order panel methods are used for the prediction and correction of the 2- and 3-dimensional wind tunnel wall effects on lifting surfaces. For each case, the practical formulations provided in the sub-sections below have been developed to calculate the low-speed potential flow fields around the multicomponent airfoils, wings or bodies. For these calculations wind tunnel walls are considered as non-lifting surfaces for both 2- and 3-dimensional cases.

Two Dimensional Method

As a result of Green's third identity, Laplace equation governing the 2D potential flow problem around a multi-element airfoil in a wind tunnel as shown in Figure 2 is reduced to the following integral equation [Katz and Plotkin, 2001].

$$\phi(p)=\phi_\infty(p)+\sum_{k=1}^{NS}\frac{1}{2\pi}\oint[\sigma(s)\ln r(s,p)+\gamma(s)\theta(s,p)]ds \quad (1)$$

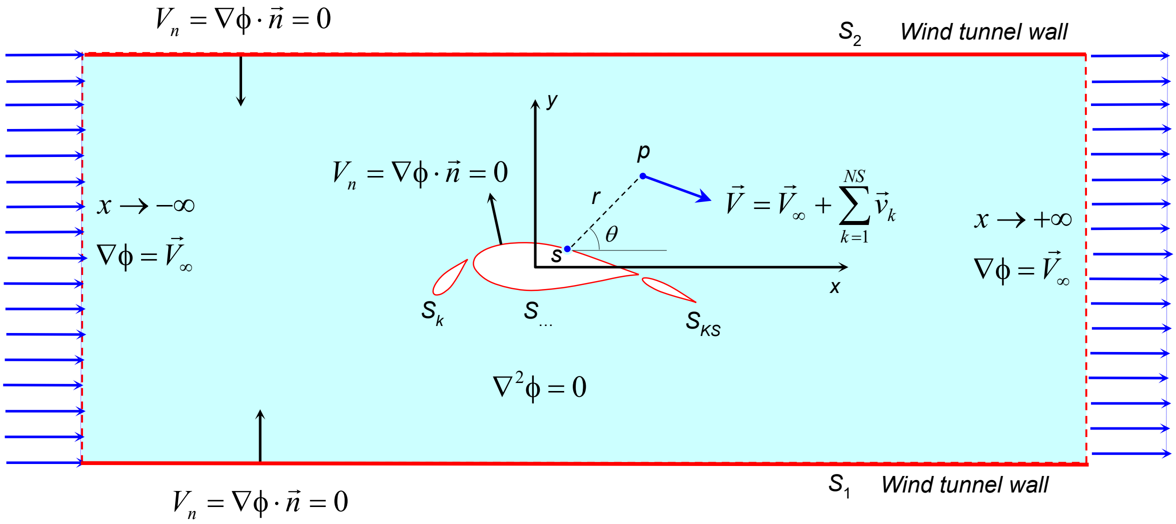

Figure 2: Potential flow problem for a multi-element airfoil in a wind tunnel

Where, *p* and *s* is any point in the flow field and on the solid surfaces, respectively; σ and γ are the unknown source and vortex strengths distributed on the solid surfaces; $\phi(p)$ is the potential value at the point *p* and $\phi_\infty(p)$ is the contribution of the free flow potential at this point; *NS* is the number of solid surfaces, including the tunnel walls.

Unknown singularity strengths in Eq. (1) are calculated by using the following equation obtained from the flow tangency condition applied at q points on the solid surfaces.

$$V_n(q)=\vec{V}_\infty\cdot\vec{n}_q+\sum_{k=1}^{NS}\frac{1}{2\pi}\oint\left[\sigma(s)\frac{\partial}{\partial n_q}(\ln r)+\gamma(s)\frac{\partial\theta}{\partial n_q}\right]ds=0 \quad (2)$$

Ones the unknowns are obtained, the tangential velocities on the solid surfaces are calculated with the following integral

$$V_t(q)=\vec{V}_\infty\cdot\vec{t}_q+\sum_{k=1}^{NS}\frac{1}{2\pi}\oint\left[\sigma(s)\frac{\partial}{\partial t_q}(\ln r)+\gamma(s)\frac{\partial\theta}{\partial t_q}\right]ds \quad (3)$$

Since the unknowns in Eq. (2) are in the integrals, the solution is difficult. In order to overcome this difficulty, the panel methods discretize the solid surface into small panels and takes the singularities out of integrals. In the method applied here, the panels are accepted as straight lines and both the source and vortex singularities are assumed constant on each panel, as shown in Figure 3.

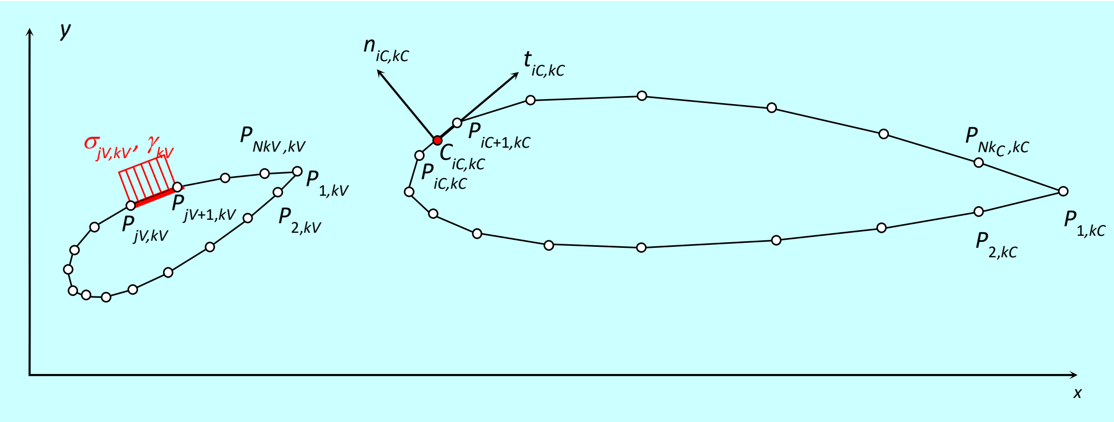

Figure 3 : Discretization applied for the present panel method

Applying the surface condition at one point at each panel N_k equation is obtained for any k^{th} surface. However, there are $2N_k$ unknown for this surface (N_k for sources and N_k for vortices). In order to reduce the number of unknowns, a convenient distribution was offered by Hess [Hess,1967]. In this method, the vortices are constant at each panel, but parabolic around the airfoil, resulting with only one unknown for the vortices on each lifting airfoil element instead N_k. In order to close the linear equations system an additional equation for each airfoil element Kutta condition is applied. Kutta condition is not necessary for the tunnel walls.
With these assumptions Eq. (1) and (2) takes the following form:

$$\sum_{kS=1}^{NS}\sum_{j=1}^{N_{kS}+1} D_{(iC,kC),(jS,kS)} X_{jS,kS} = R_{iC,kC} \qquad (iC = 1,2,\ldots,N_{kC}+1); \quad kC = 1,\ldots,KP \tag{4}$$

$$V_{t_{iC,kC}} = Q_{iC,kC} + \sum_{kS=1}^{NS}\sum_{jV=1}^{N_{kS}+1} E_{(iC,kC),(jS,kS)} X_{jS,kS} \tag{5}$$

Where, $X_{jS,kS}$ are the singularity strengths on the surface kS, including N_{kS} source and a vortex. $R_{(iC,kC)}$ and $Q_{(iC,kC)}$ is the normal and tangential contribution, respectively, of the free flow at the control point (iC,kC). And $D_{(iC,kC),(jS,kS)}$ and $E_{(iC,kC),(jS,kS)}$ is normal and tangential velocities, respectively, induced by the unit strength singularity on the panel (iS,kS) at the control point (iC,kC) to be calculated by the following integrals:

$$E_{(iC,kC),(jS,kS)} = \frac{1}{2\pi}\int_{P_{(jS,kS)}}^{P_{(jS,kS)+1}} \frac{\partial}{\partial t_i}(\ln r)\, dt_j \tag{6}$$

$$D_{(iC,kC),(jS,kS)} = \frac{1}{2\pi}\int_{P_{(jS,kS)}}^{P_{(jS,kS)+1}} \frac{\partial}{\partial n_i}(\ln r)\, dt_j \tag{7}$$

For each airfoil, $N_{kC+1}{}^{th}$ equation is obtained from Kutta condition. The linear equations system shown in matrix form in Figure 4 can be solved for the singularity strengths by using Gauss elimination method. It should be mentioned that the last row of each sub-matrix of non-lifting elements replaced by zero except the diagonal term, which is 1.

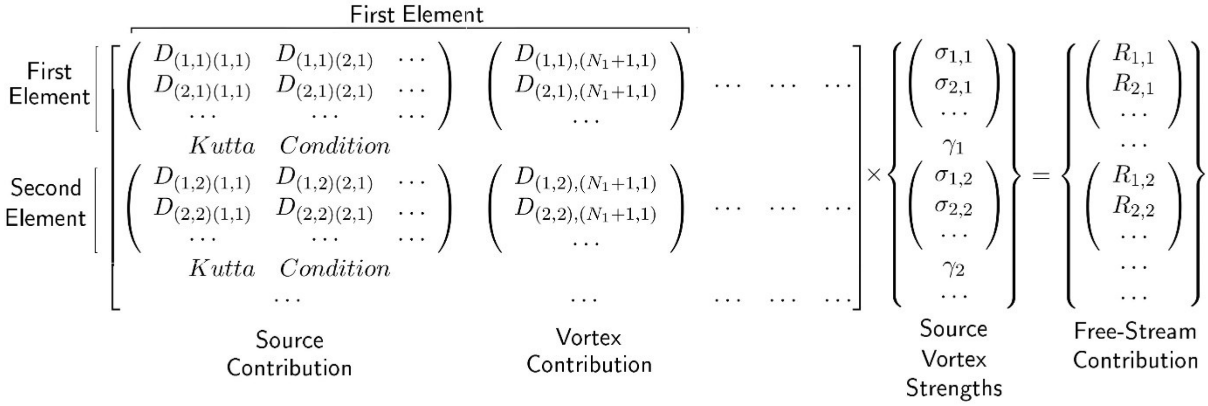

Figure 4: Influence Coefficients Matrix Structure for Normal Velocities of a Multi-Element System

The tangential velocities at control points are calculated by Eq. 5, or by the matrix equality shown in Figure 5.

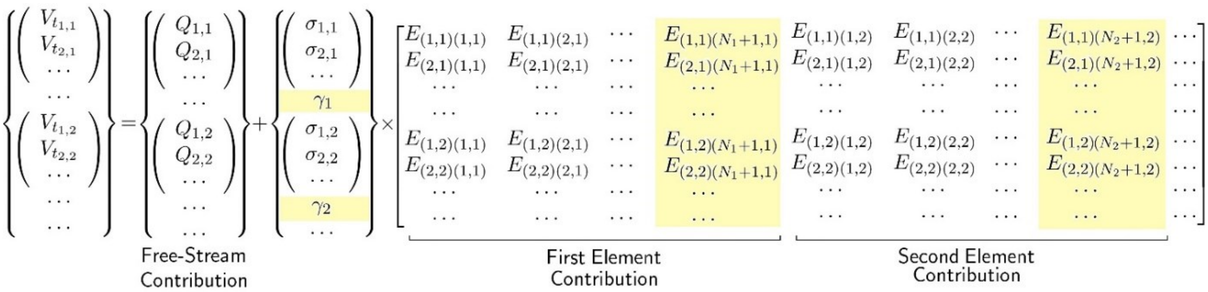

Figure 5: Total Tangential Velocities in Matrix From

A Visual Basic program is developed for the application of the method. Main structure of the program is given in Figure 6.

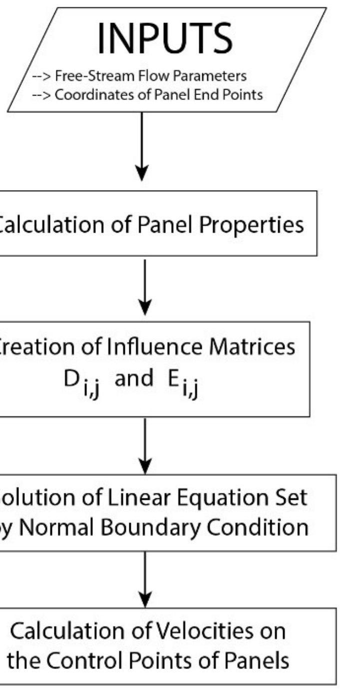

Figure 6: Flow Diagram of The 2D Program

Aerodynamic coefficients of *k'th* lifting element can be calculated as follows

$$c_x = \sum_{i=1}^{NI} (1 - Cp_i) \times ds_i \times \zeta_{x_i} \tag{8}$$

$$c_z = \sum_{i=1}^{NI} (1 - Cp_i) \times ds_i \times \zeta_{z_i} \tag{9}$$

$$c_l = (c_z \times \cos\alpha - c_x \times \sin\alpha) \qquad c_d = (c_x \times \cos\alpha + c_z \times \sin\alpha) \tag{10}$$

Where ds_i is the length of i'th panel, ζ_i is its unit normal vector. And Cp_i is the pressure coefficient on this panel to be calculated as

$$C_{p,i} = 1 - \left(\frac{V_{t,i}}{V_\infty}\right)^2 \tag{11}$$

Three Dimensional Method

For the 3D flows around wings both in isolated case and in wind tunnel, Vortex Ring Method is used to model the lifting surfaces. Non-lifting bodies are modelled by source panels. For the modelling of wind tunnel walls two options are possible, Vortex Ring Method or 3D source panel method, in this study. Formulations of these methods are provided in the following sections.

Vortex Ring Method: VRM is an alternative application of the Vortex Lattice Method (VLM). In VLM a finite wing is divided into small panels both in spanwise and chordwise directions, and each panel is represented by a horse-shoe vortex; its bound vortex part takes place on the quarter chord line of the panel. The trailing parts of each horse-shoe vortex follow the surface up to trailing edge then go to infinity in the direction of the free flow. In VRM, bound vortices on adjacent panels and segments of two trailing vortices between two panels are collected in to a quadrilateral ring vortex as shown in Figure 7. And a horse-shoe vortex behind the trailing edge represents the wake.

The unknowns of this problem are strengths of the ring vortices to be obtained by applying the flow tangency boundary condition at control points on each panel. The control points are the centroids of the ring vortices.

Since the essentials of the method for a single wing is given by [Katz and Plotkin, 2001] in detail, here only the development of the formulation for a multi-lifting surface with wind tunnel wall is given.

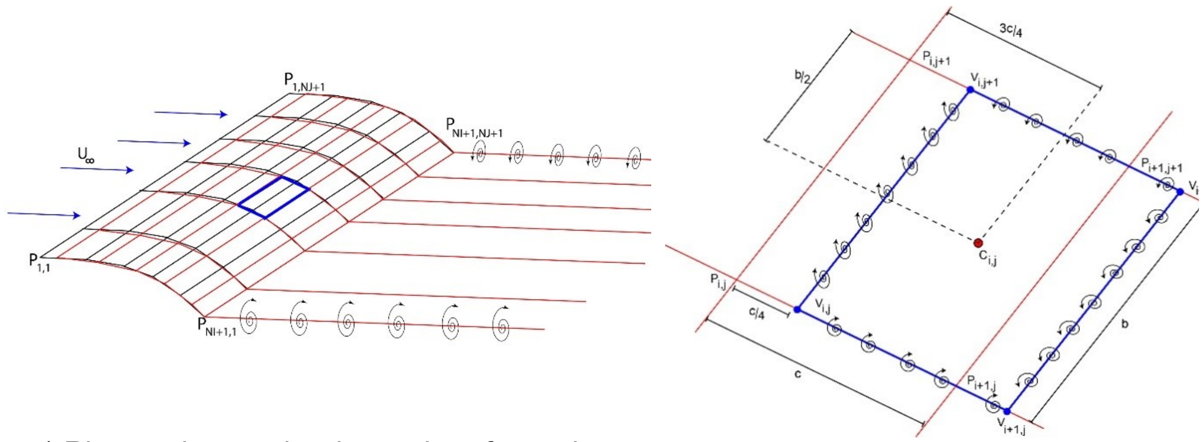

a) Ring vortices and wake vortices for a wing b) Ring vortex for a panel

Figure 7: System of ring vortices representing a wing

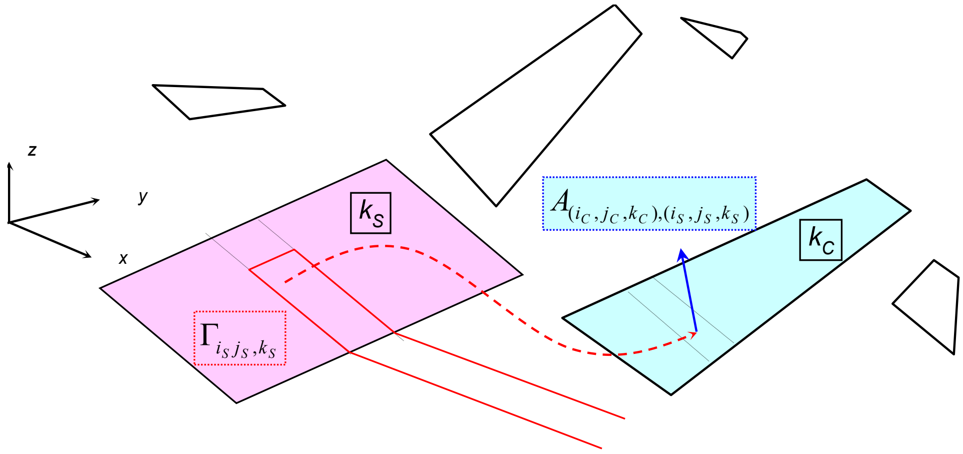

Figure 8: Application of the boundary condition in a multi-wing system

Applying the surface boundary condition for a system of multi-lifting surfaces shown in Figure 8 the following equations system is obtained:

$$\sum_{kS=1}^{NS}\sum_{iS=1}^{NI_{kS}}\sum_{jS=1}^{NJ_{kS}} B_{(iC,jC,kC),(iS,jS,kS)}\Gamma_{iS,jS,kS} = R_{iC,jC,kC} \qquad \begin{pmatrix} iC = 1,2,...,NI_{kC} \\ jC = 1,2,...,NJ_{kC} \end{pmatrix}; \quad (kC = 1,...,KS) \tag{12}$$

Where, $\Gamma_{iS,jS,kS)}$ are the strength of vortex rings on the surface *kS*. $R_{(iC,jC,kC)}$ is the normal contribution of the free flow at the control point (*iC,jC,kC*) on lifting surfaces. Coefficient $B_{(iC,jC,kC),(jS,jS,kS)}$ is the normal component of the velocity induced by the unit strength vortex rings on panel (*iS,jS,kS*) to control point (*iC,jC,kC*), to be calculated by the following equation:

$$B_{(iC,jC,kC),(iS,jS,kS)} = \vec{v}_{(iC,jC,kC),(iS,jS,kS)} \cdot \vec{\zeta}_{(iC,jC,kC)} \tag{13}$$

Where $\vec{v}_{(iC,jC,kC),(iS,jS,kS)}$ is the velocity vector induced by vortex rings on panel (*iS,jS,kS*) to control point (*iC,jC,kC*). $\vec{\zeta}_{(iC,jC,kC)}$ is the unit normal vector of panel (*iC,jC,kC*). Strength of vortex rings can be calculated by solving Eq. (12). Then aerodynamic forces of panel (*iC,jC,kC*) can be calculated by using the following vector form of the Kutta-Joukowski theorem for lift.

$$\Delta\vec{F}_{(iC,jC,kC)} = \rho \cdot \vec{V}_{(iC,jC,kC)} \times (\Gamma_{(iC,jC,kC)} \cdot \Delta\vec{s}_{(iC,jC,kC)}) \tag{14}$$

Where ρ is the fluid density, $\vec{V}_{(iC,jC,kC)}$ is velocity induced by all vortex rings on the midpoint of bound vortex segment of panel (*iC,jC,kC*) and $\Delta\vec{s}_{(iC,jC,kC)}$ is the line vector take place on the bound vortex of the panel (*iC,jC,kC*).

<u>Source Panel Method:</u> As mentioned in previous sections, 3D Source Panel method is used for non-lifting bodies and wind tunnel walls. 3D panel methods use generally two types of singularities; source distribution and doublet distribution. For the current work, only source distribution is used for the non-lifting components.
As in the 2D Hess-Smith method, Laplace equation governing the 3D potential flow problem around a multi-element body as shown in Figure 9 is reduced to Eq. (15) [Katz and Plotkin, 2001].

$$\phi(p) = \phi_\infty(p) + \frac{1}{4\pi}\oint[\frac{\sigma(q)}{r(P,q)}]ds \tag{15}$$

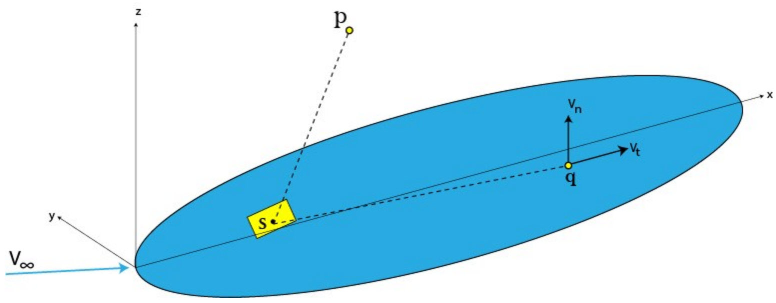

Figure 9: Velocity potential at point P

Where, *p* and *q* is any point in the flow field and on the solid surfaces, respectively; σ is the unknown source strengths distributed on the solid surfaces; $\phi(p)$ is the potential value at the point *p* and $\phi_\infty(p)$ is the contribution of the free flow potential at this point; *NS* is the number of solid surfaces.

Unknown singularity strengths in Eq. (15) are calculated by using the following equation obtained from the flow tangency condition on the solid surfaces

$$V_n(q) = \vec{V}_\infty \cdot \vec{n}_q + \sum_{k=1}^{NS} \frac{1}{4\pi}\oint \frac{\partial}{\partial n_q}\left[\frac{\sigma(s)}{r(s,q)}\right]ds = 0 \tag{16}$$

$$V_t(q) = \vec{V}_\infty \cdot \vec{t}_q + \sum_{k=1}^{NS} \frac{1}{4\pi}\oint \frac{\partial}{\partial t_q}\left[\frac{\sigma(s)}{r(s,q)}\right]ds \tag{17}$$

Since the unknowns in Eq. (16) are in the integrals, the solution is difficult. Likewise 2-dimensional solution, the panel methods discretize the solid surface into small panels and takes the singularities out of integrals as illustrated in Figure 10. In this method, the panels are considered as flat quadratic plates and the source distribution over each panel is considered as constant.

With this discretization, Eq. (16) can be rewritten as following form

$$\sum_{kS=1}^{NB}\sum_{iS=1}^{NI(kS)}\sum_{jS=1}^{NJ(kS)} B_{(iC,jC,kC),(iS,jS,kS)} X_{(iS,jS,kS)} = R_{iC,jC,kC} \tag{18}$$

$$V_{t_{iC,jC,kC}} = Q_{iC,jC,kC} + \sum_{kS=1}^{NB}\sum_{iS=1}^{NI(kS)}\sum_{jS=1}^{NJ(kS)} A_{(iC,jC,kC),(iS,jS,kS)} X_{iS,jS,kS} \tag{19}$$

$$iC = 1,...,NI(kC) \qquad jC = 1,...,NJ(kC) \qquad kC = 1,...,NB$$

Where, $X_{(iS,jS,kS)}$ are the singularity strengths on the surface *kS*, $R_{(iC,kC)}$ and $Q_{(iC,kC)}$ is the normal and tangential contribution, respectively, of the free flow at the control point (*iC,jC,kC*). And $B_{(iC,jC,kC),(iS,jS,kS)}$ and $A_{(iC,jC,kC),(iS,jS,kS)}$ are normal and tangential velocities, respectively, induced by the unit strength singularity on the panel (*iS,jS, kS*) at the control point (*iC,jC,kC*) to be calculated by the following integrals:

$$A_{(iC,jC,kC),(iS,jS,kS)} = \iint_{s_{(iS,jS,kS)}} \frac{\partial}{\partial t_{(iC,jC,kC)}} \left[\frac{1}{r(S_{(iS,jS,kS)},q)} \right] ds \tag{20}$$

$$B_{(iC,jC,kC),(iS,jS,kS)} = \iint_{s_{(iS,jS,kS)}} \frac{\partial}{\partial n_{(iC,jC,kC)}} \left[\frac{1}{r(S_{(iS,jS,kS)},q)} \right] ds \tag{21}$$

Eq. (20) and (21) can be solved by using Bousquet formulation [Bousquet, 1982].

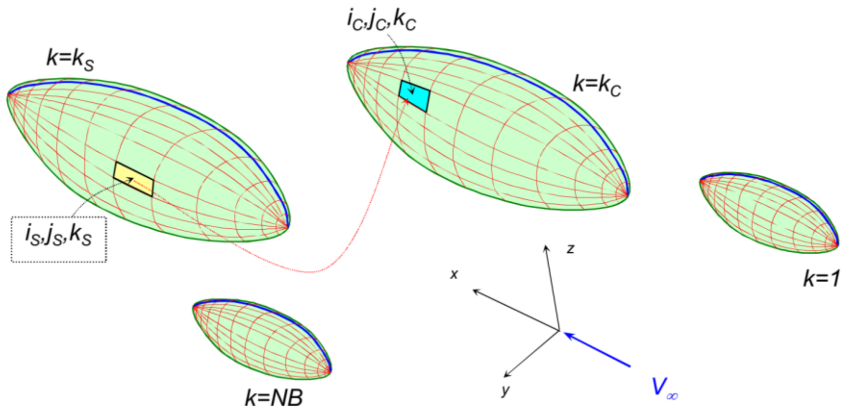

Figure 10: Application of boundary condition in a multi-element body system [Yukselen, 2017]

The program developed for 3-dimensional wind tunnel solution is using both VRM and source panel method for lifting and non-lifting surfaces. Therefore, the solution matrix must be formed with both vortex ring's influences and source panel influences. The flow diagram of 3-dimensional program is given Figure 11.

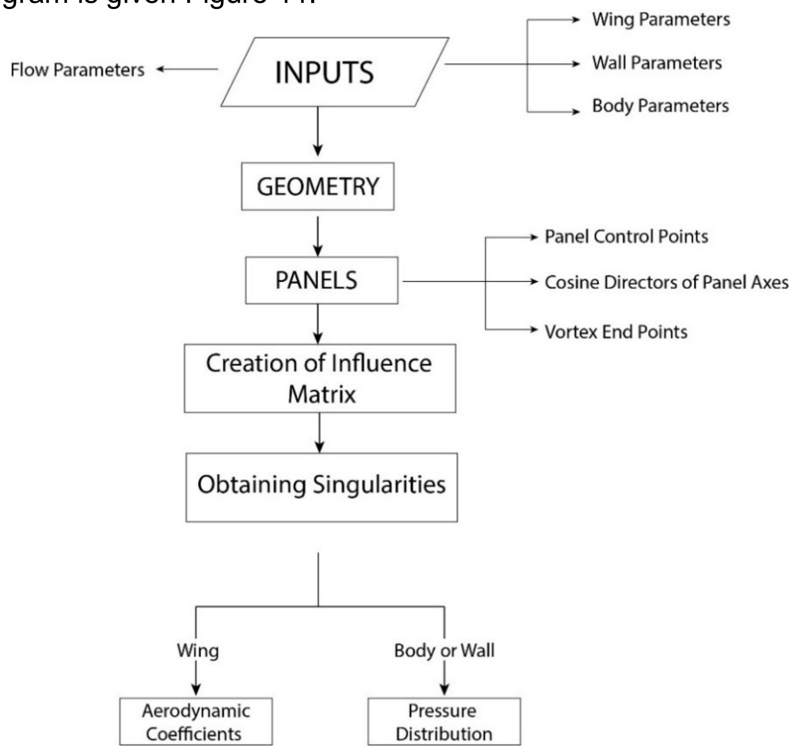

Figure 11: Flow Diagram of 3D Program

VALIDATION

In order to ensure that the method and the developed computer programs for the prediction of wind tunnel wall effects work correctly, some validation analyzes are performed.
First the 2-dimensional code is tested for the ground effect on a single-element airfoil by solving this problem for two equivalent cases shown in Figure 12: first one for an airfoil with its image, and the second one for the same airfoil with a straight line representing the tunnel wall.

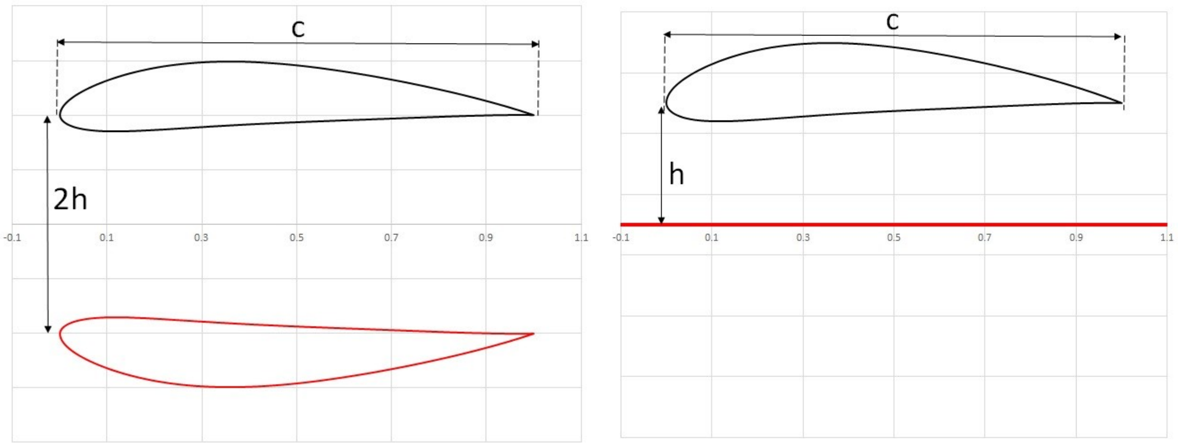

a) Airfoil and its image b) Airfoil and a straight line

Figure 12: 2D test case for ground effect on a single element NACA4412 airfoil

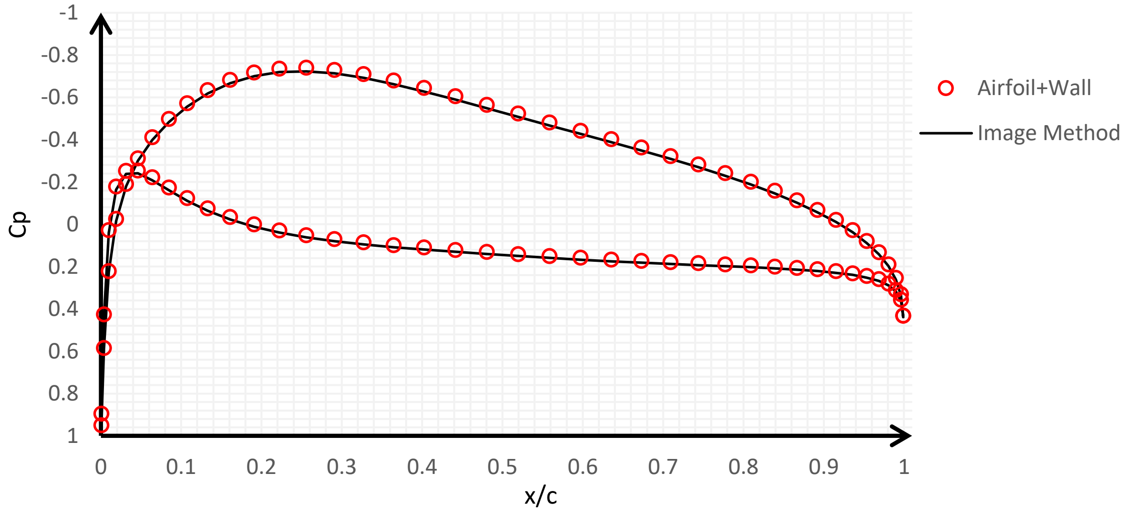

Figure 13: Pressure Distribution on the NACA4412 airfoil in ground effect with h/c = 0.5

For the two cases pressure distribution around a NACA 4412 airfoil are calculated and compared in Figure 13. The results are nearly the same. This means that a straight line can be easily used instead of the airfoils image to investigate the wall effect on the airfoil. This conclusion is important especially for the investigation of tunnel wall effects. Because, if the images method is used for this problem, infinite number of images of the airfoil are necessary to represent the effects of both lower and upper tunnel walls. This complicates the solution of the problem. However, it is simply possible to use two straight walls representing the upper and lower walls of the tunnel, instead of so many images of the airfoil.

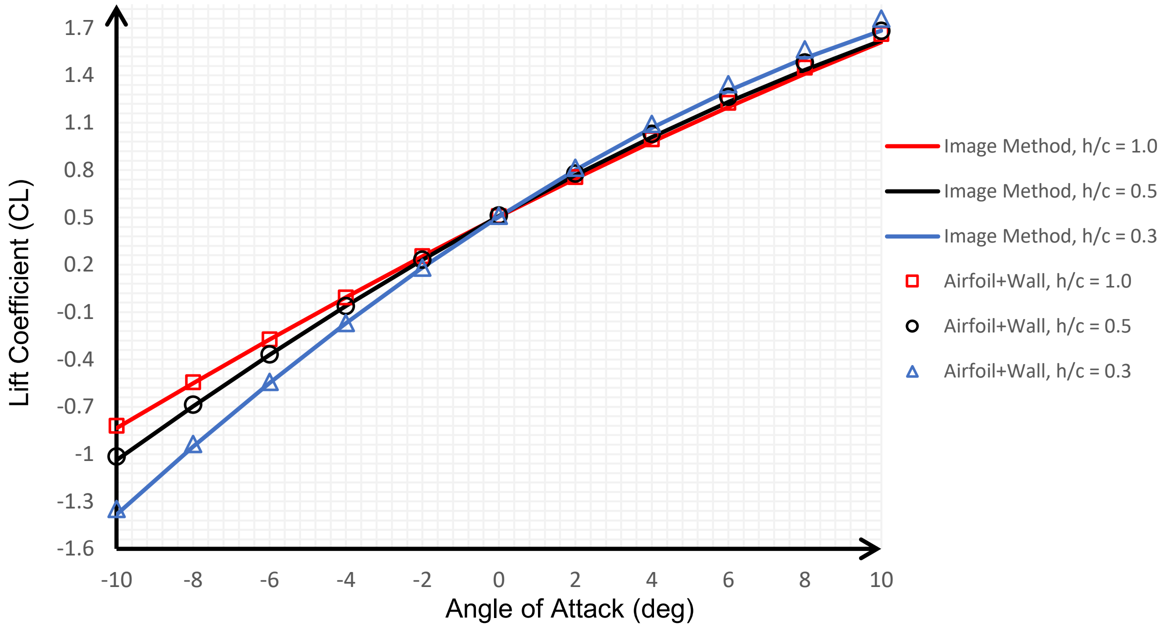

Figure 14: Lift coefficient vs angle of attack of NACA4412 airfoil with various tunnel heights

In Figure 14, lift coefficients of NACA4412 airfoil is given with different angle of attacks in various *h* values which is the vertical distance between leading edge point of airfoil and the straight line.

The code developed for 3-dimensional case also is tested for ground effect similar to 2D application by considering two equivalent cases: first one for a wing with its image with respect to horizontal plane, and the second one for a wing with a flat plate which is used to model wind tunnel wall with constant source distribution. The wing has 10 aspect ratio with a rectangular planform and NACA4412 is preferred for the wing's airfoil. The width of the flat plate is chosen as 5 times of wing's span and its length is 10 times of wing's chord.

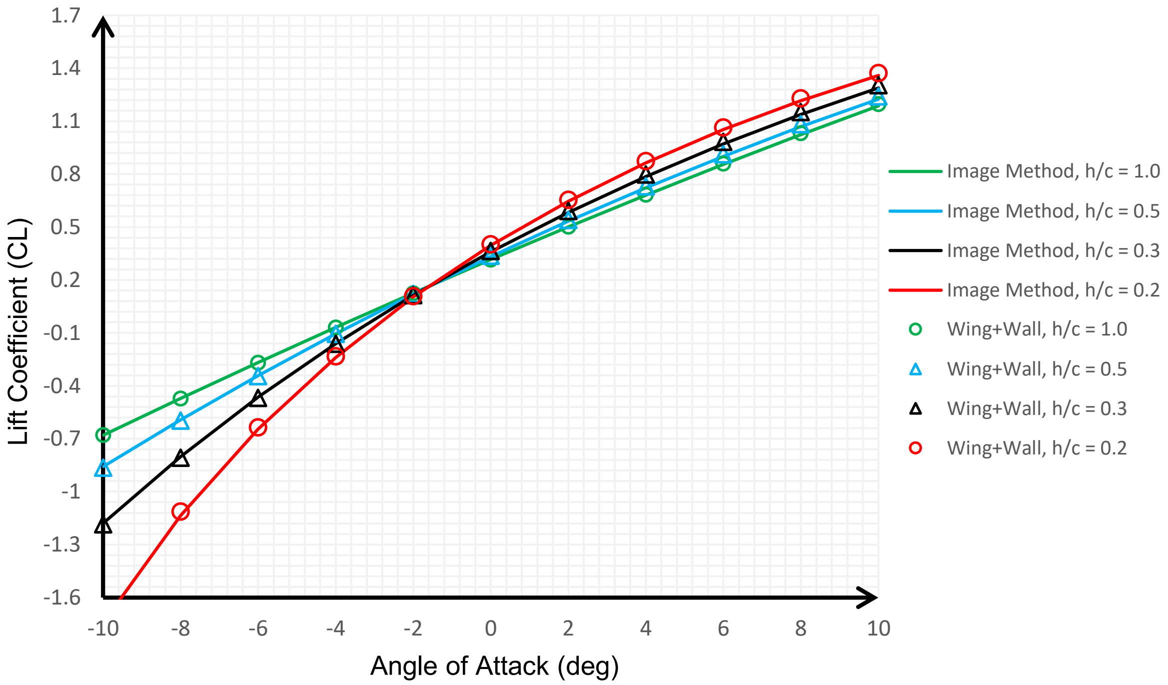

Figure 15: Lift coefficients for two cases

For the two cases, lift coefficients are calculated for several angles of attack and several values of h/c ratio. Compared results in Figure 15 are nearly the same. Here, *h* is the half distance between two wing for first case, and the distance between wing and flat plate for the second case. *c* is the chord length of the wing. As the *h/c* decreases, the lift graph becomes non-linear. Finally, the reflection test is applied for the bodies. Velocity distribution around a sphere in x-direction (flow direction) is examined for two equivalent cases: first one for a sphere with its image with respect to horizontal plane, and the second one for a sphere with a flat plate which is used to model wind tunnel wall. The flat plate is considered as a square and the dimensions of the square were chosen to be 10 times the diameter of the sphere.

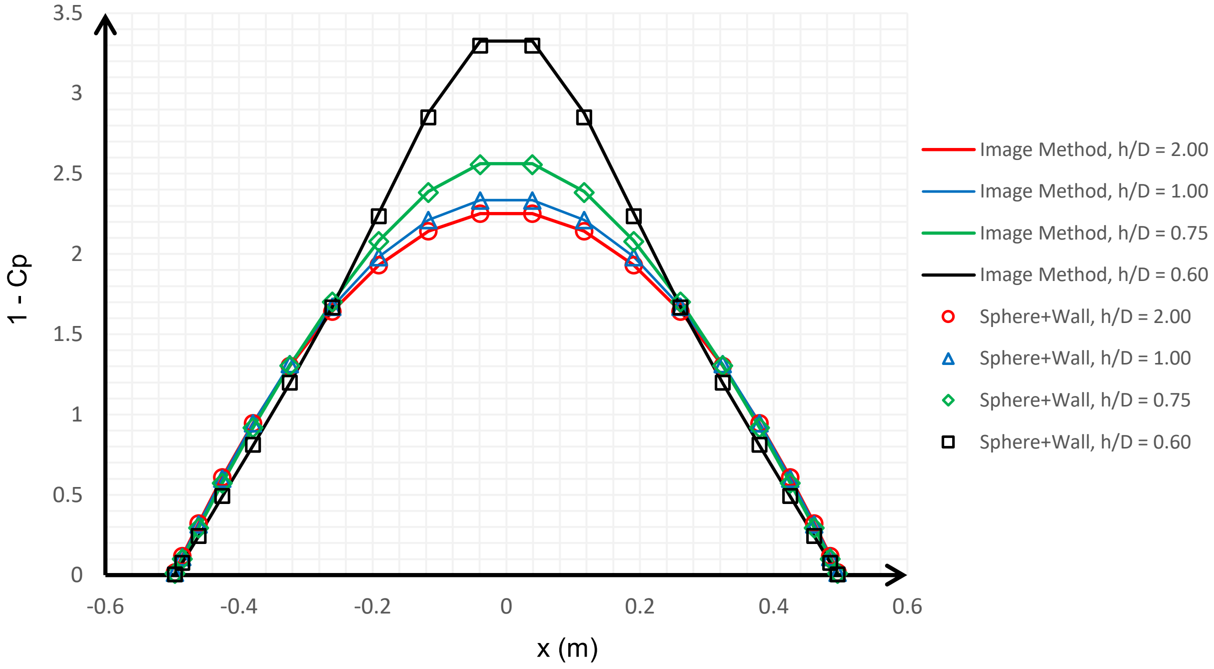

Figure 16: Velocity distribution over a sphere with various heights

In Figure 16, *D* is the diameter of the sphere and *h* is the vertical distance between horizontal flat plate and center of the sphere. From these validation tests, it can be seen that the panel method is a confidential method for the prediction of wall effects.

APPLICATIONS FOR WALL EFFECTS

Validation tests in the previous section shows that the developed computer programs, using a flat surface representing the ground, for 2- and 3-D potential flow calculations around airfoils and wings in ground effect work correctly. In this section, these programs are applied for some examples related to wind tunnel wall effects, and the results are compared with those of classical methods, previous studies and the experimental data.

First example is on a NACA0012 airfoil at 2 degrees angle of attack. By using the 2D code, lift coefficients are calculated in free airflow and in wind tunnel for various values of tunnel height/airfoil chord length ratio. The ratio between the lift coefficients in free flow and in wind tunnel is obtained for various tunnel heights. Variation of the normalized lift coefficient with h/c ratio is given in Figure 17. These results are compared with those of obtained with the methods of Abbot and Pope given in [Abdullah, 2015]. The results are almost the same.

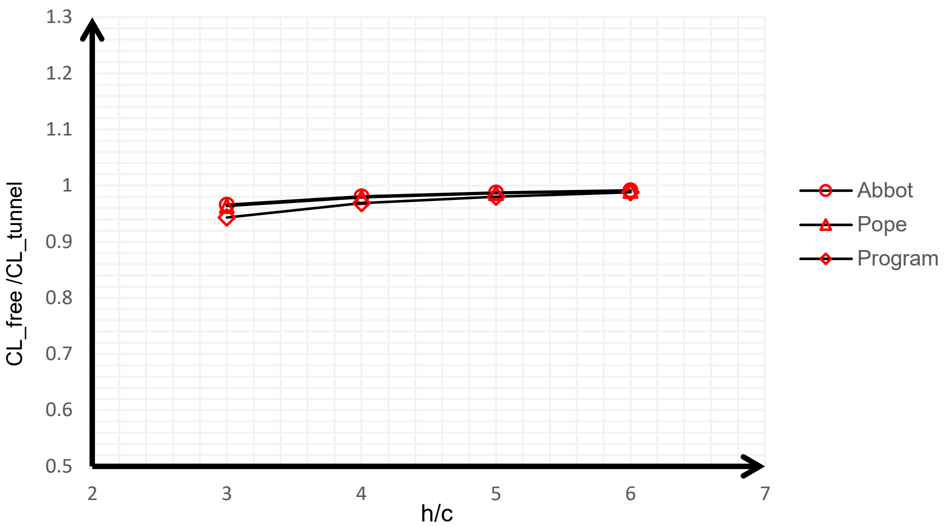

Figure 17: Lift coefficient correction comparison with classical methods

In the second example, the flow around NACA 64A010 and NACA 23012 airfoils placed at the center of wind tunnel are analyzed for various blockage ratios represented by thickness/tunnel height ratio (*t/h*) and the schematics of the example is given in Figure 18. Distribution of pressure coefficient over airfoils are presented in Figure 19 and Figure 20. The results are compared with the results obtained by a linear vortex panel method in [Ojha and Shevare, 1985]. Two groups of results are very close to each other.

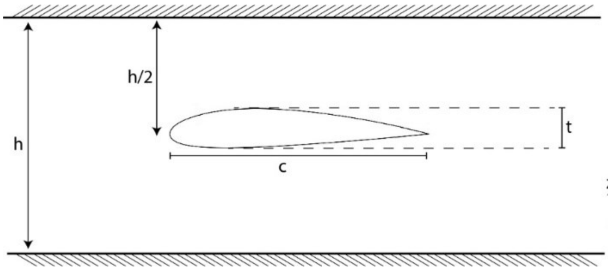

Figure 18: Dimensions of the airfoil and wind tunnel [Ojha and Shevare, 1985]

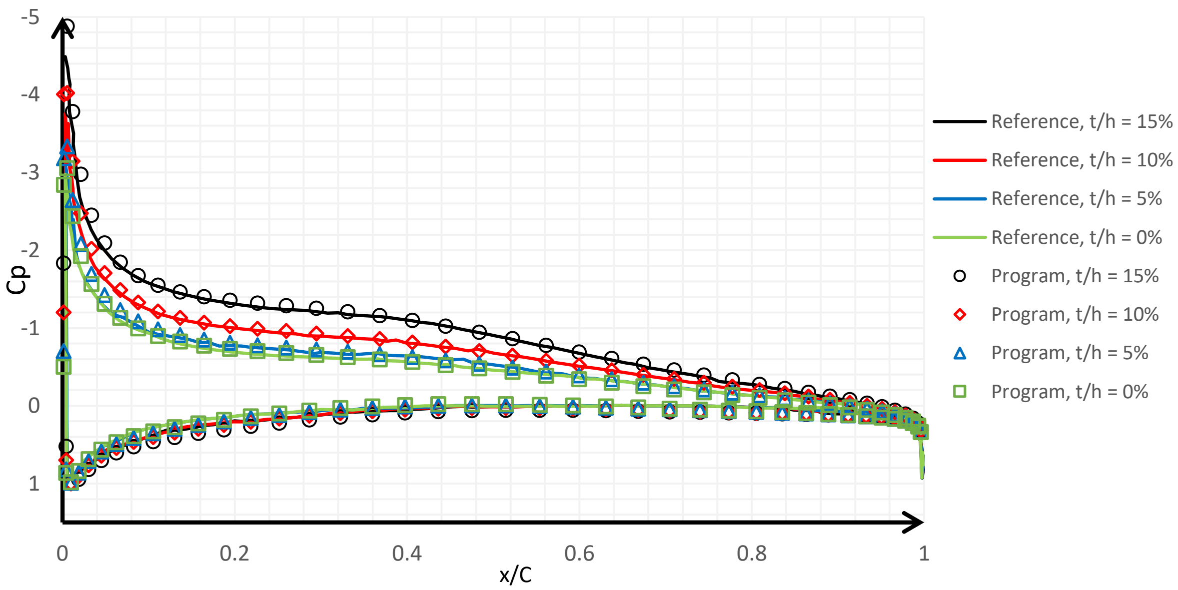

Figure 19:Pressure coefficient comparison of NACA 64A010 airfoil in wind tunnel at 5 degree angle of attack with various t/h values

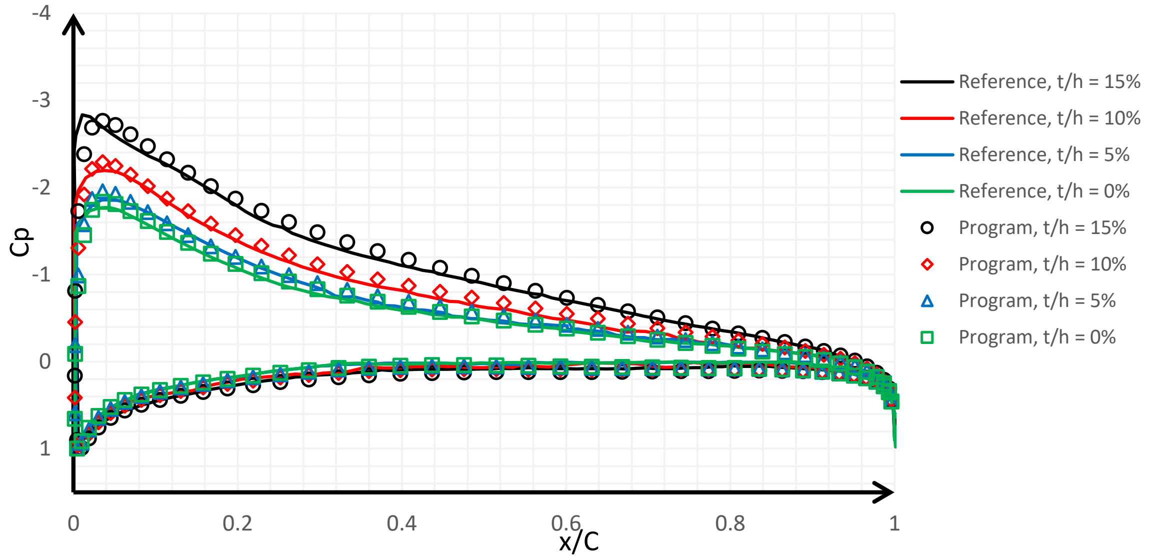

Figure 20: Pressure coefficient comparison of NACA 23012 airfoil in wind tunnel at 5 degree angle of attack with various t/h values

Third example is on a multi-element airfoil show in Figure 21. In this combination the main element is a NACA4412 airfoil and the flap is a NACA4415 airfoil.

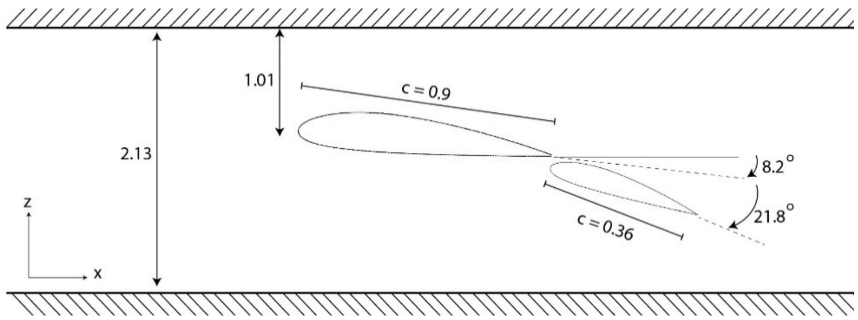

Figure 21:Dimensions of the multi-element airfoil and wind tunnel [Browne and Katz, 1990]

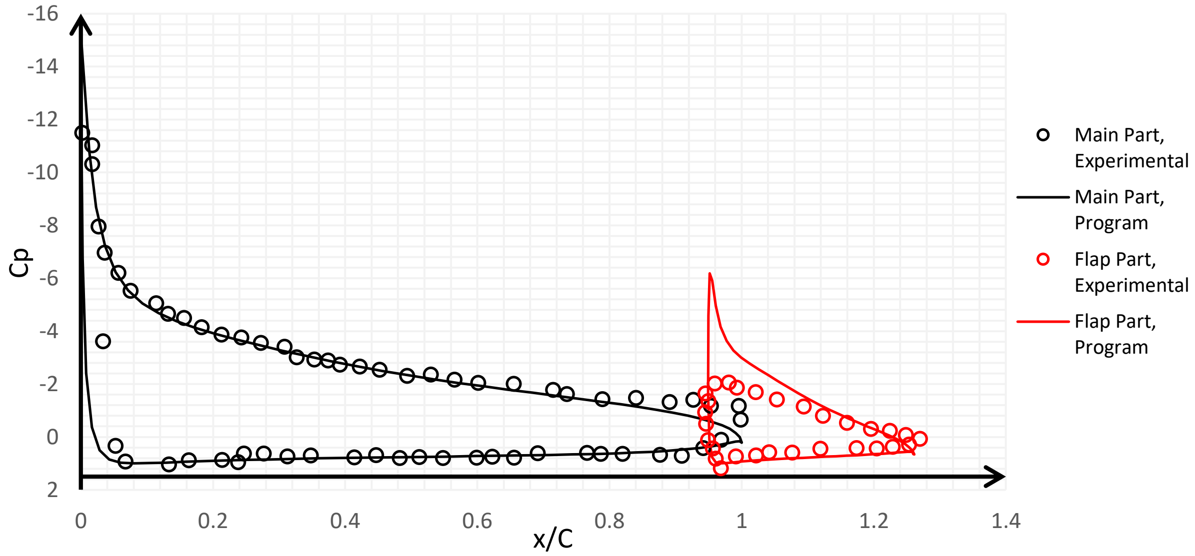

Figure 22: Pressure coefficient distribution over multi-element airfoil in wind tunnel

Pressure distribution around this multi-element airfoil is presented in Figure 22, and compared by the experimental results given in [Browne and Katz, 1990]. Pressure distribution obtained from our code is almost the same with the experimental data except the leading edge of flap and trailing edge of main part. This difference is caused by a small trailing edge separation which is not considered in our potential flow based code.

Figure 23 shows the pressure distributions on the upper and lower tunnel walls. The differences between the theoretical and experimental results are also due to potential flow approximation of our code.

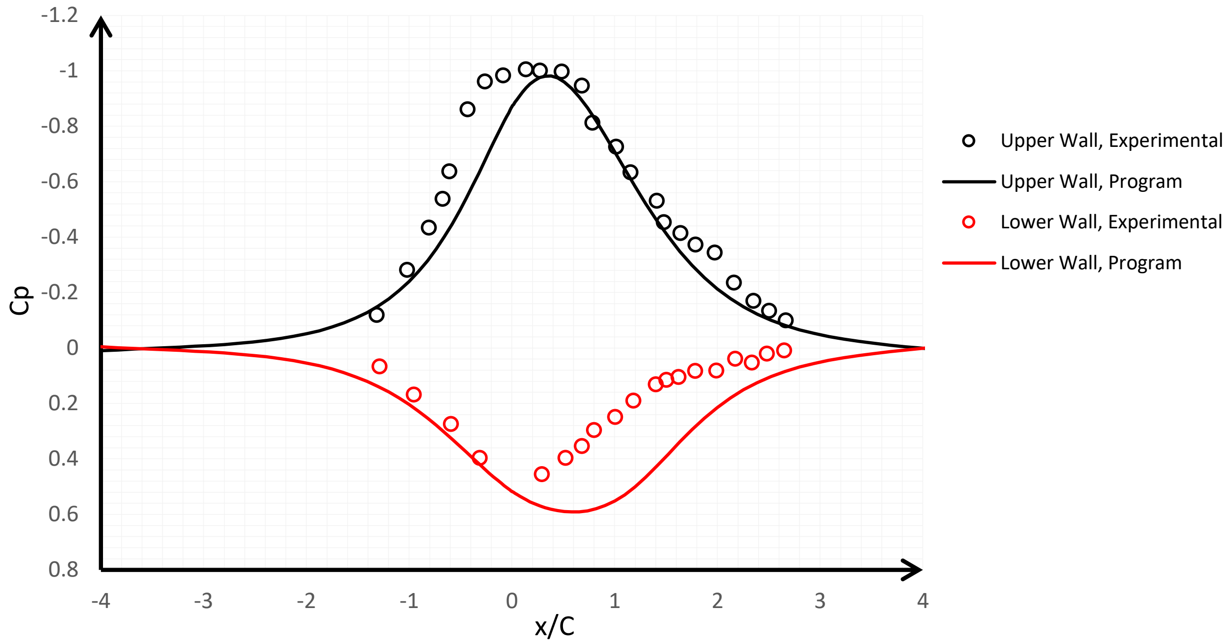

Figure 23: Pressure coefficient distribution over wind tunnel walls

As an example for 3D case, the flow around a sphere of 15-inch diameter in a wind tunnel test section of 30x43 inches dimensions. The results are compared in Figure 24, with the results of a source panel method and the experimental results for 6.5 Reynolds number given in [Hackett, Wilsden and Lilley, 1979]. Our results are very close to the results of previous theoretical method and also to the experimental results except aft of the sphere where the viscosity effects are important.

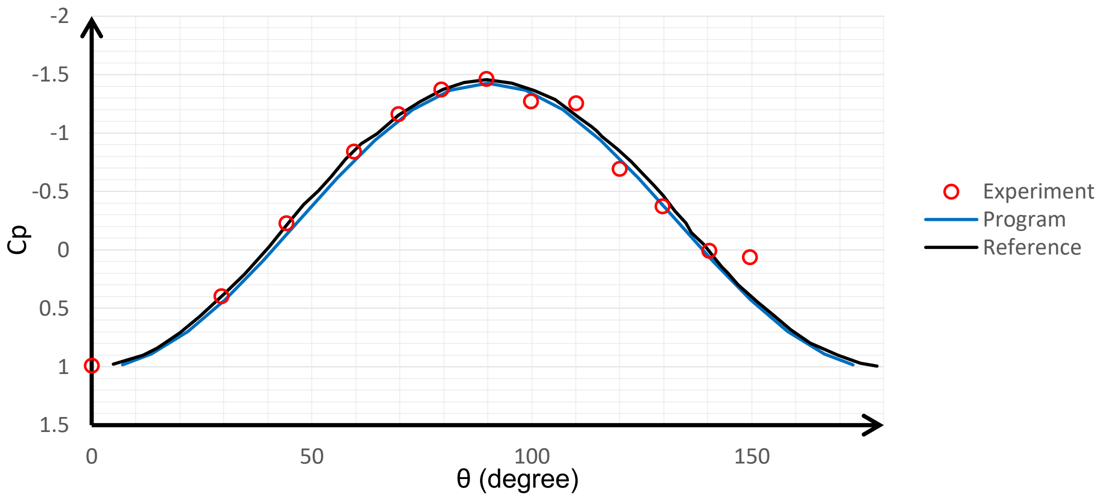

Figure 24: Pressure coefficient distribution around 15inch sphere in flow direction

Wall Effect Predictions

The wind tunnel wall effect can be evaluated as the difference between the results for a body in free flow and in wind tunnel. As an example, a NACA 4412 airfoil placed in 2D wind tunnel is analyzed for various angles of attack and tunnel heights. The differences between the lift coefficients obtained in free flow case and in wind tunnel case are shown in Figure 25. The results show that the wall effect on airfoil lift coefficient is increase with both, increasing angle of attack and the ratio of chord/tunnel height

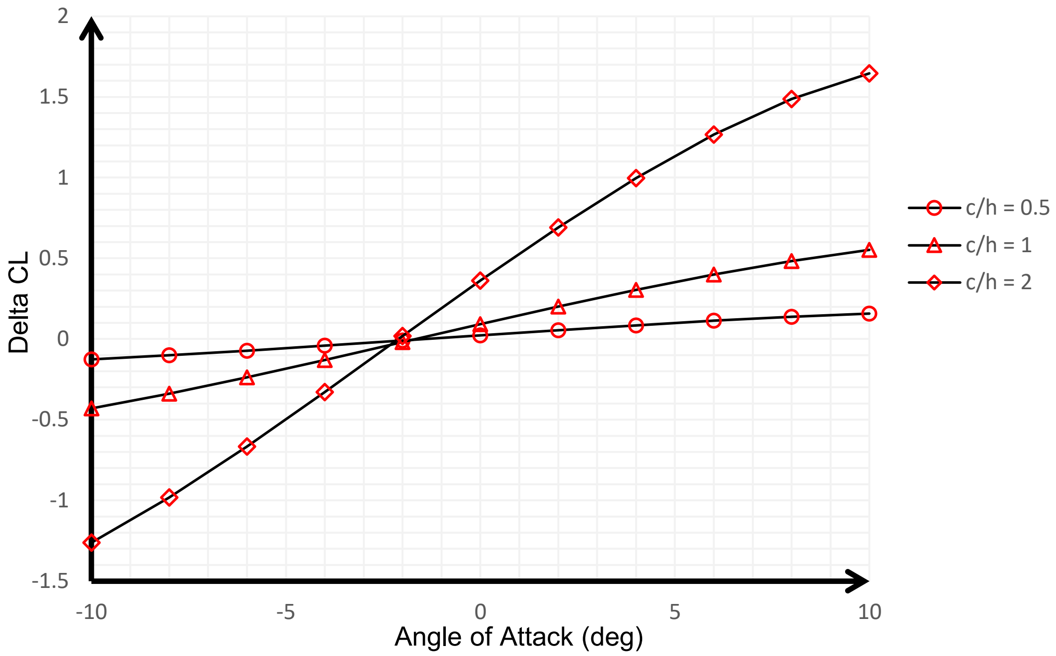

Figure 25: Lift coefficient difference between wind tunnel and isolated case

As an example for 3D case, wall effects on lift coefficients of a wing having an aspect ratio 10 and a cross section NACA 4412 airfoil shown in Figure 26 are calculated.

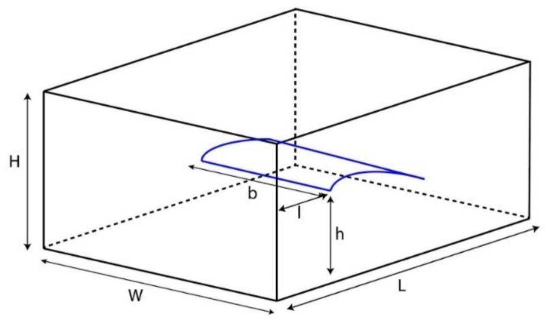

Figure 26: Schematics of wind tunnel and rectangular wing

In Figure 27, width of the tunnel was kept constant as 2 times of wing span and height of the tunnel was kept constant as 3 times of chord of the wing in Figure 28

The differences between the lift coefficients obtained in free flow and in wind tunnel at various angle of attacks is presented in Figure 27 for various H/c (tunnel height/wing chord length) ratios with a constant tunnel width of 2 times the wing span and in Figure 28 for various W/b (tunnel width/wing span) ratio with constant tunnel height of 4 times the wing chord length.

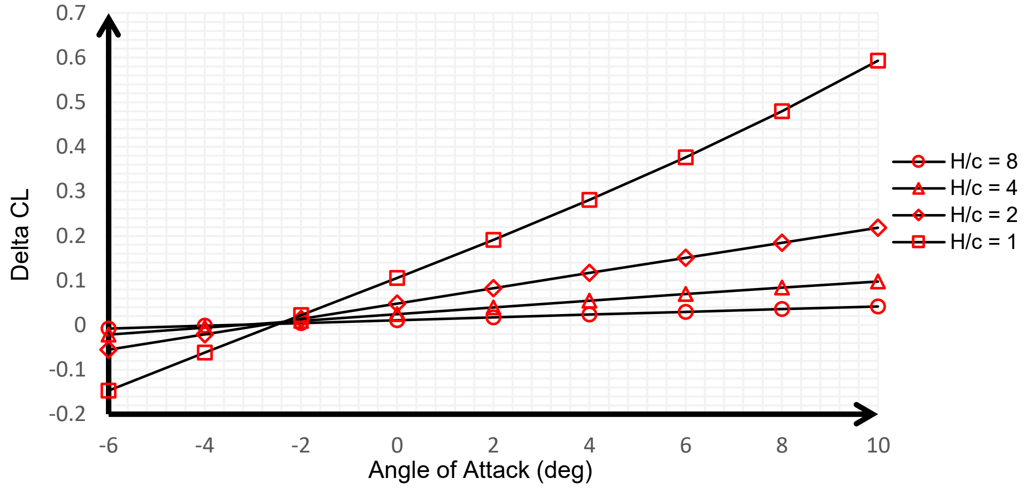

Figure 27:Lift coefficient change with various tunnel heights

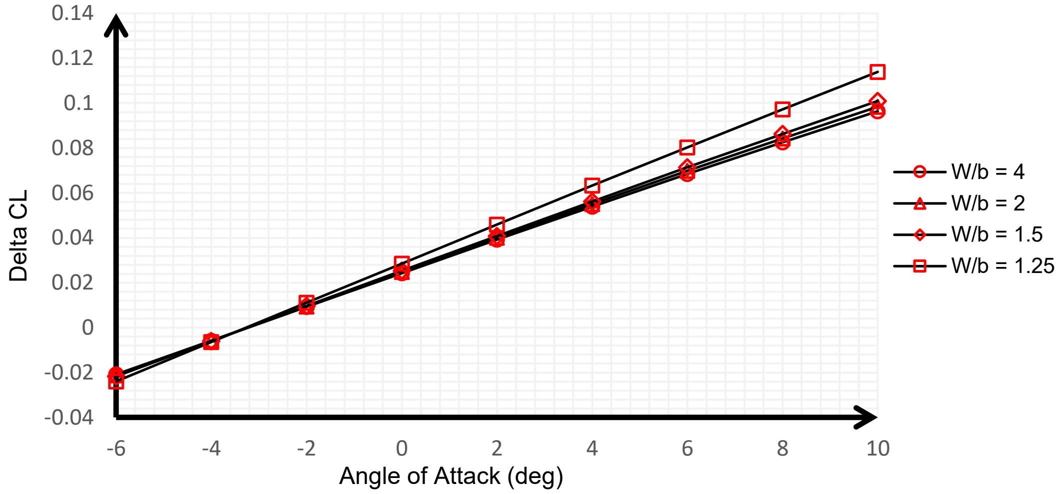

Figure 28: Lift coefficient change with various tunnel widths

The results show that the wall effects increase with both, angle of attack and H/c or W/b ratios. All analyzes were performed on a computer which has 2.4 Ghz CPU and 12 Gb RAM. Solution time with respect to panel number is given Figure 29.

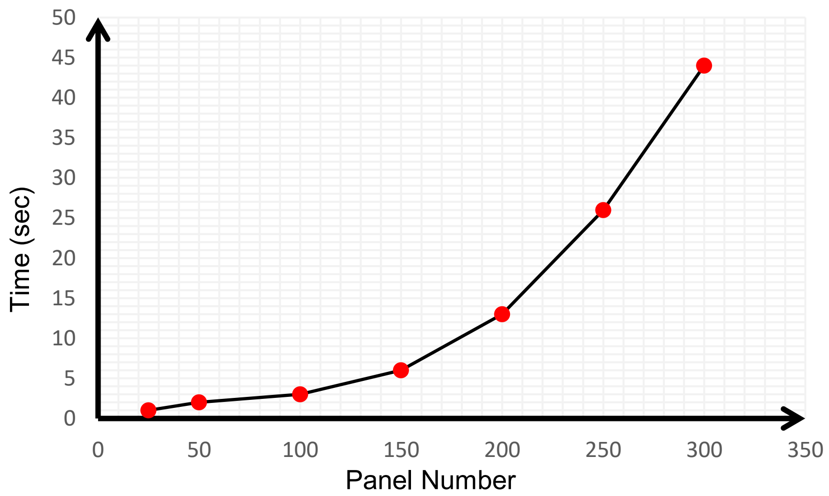

Figure 29: Solution time according to panel number

CONCLUSION

From test applications and results, it can be concluded that panel methods have sufficient accuracy for the prediction of wall effects. It must be noted that flow solution given in this article is not valid for separated flow. However, the program can produce acceptable results at the small and moderate angles of attack. In addition, less solution time of the panel methods make them stand out. It can be seen as future work that panel methods can be preferred for wind tunnel design and optimization.

References

Abdullah T. A. (2015), “Two-dimensional wind tunnel measurement corrections by the singularity method,” *Teh. Vjesn. Gaz.*, vol. 22, no. 3, pp. 557–565, 2015.

Allmaras S.R. (1986), "On Blockage Corrections for Two-Dimensional Wind Tunnel Tests Using the Wall Pressure Signature Method", NASA Ames Research Center, NASA-TM-86759.

Bousquet J. (1982), “Methode des Singularites”, Theorie et Applications, École Normale Supérieure de L'Aéronautique et de l'Espace, Course Notes, pp. 5.5.

Browne L. and Katz J. (1990), "Application of Panel Methods to Wind-Tunnel Wall Interference Corrections", 28th AIAA Aerospace Sciences Meeting.

Garner H. C., Rogers E. W. E., Acum W. E. A. and Maskell E. C. (1967) *Subsonic wind tunnel corrections*, Advisory Group for Aerospace Research and Development, North Atlantic Treaty Organization.

Hackett J. E., Wilsden D. J. and Lilley D. E. (1979), “Estimation of Tunnel Blockage from Wall Pressure Signatures: A Review and Data Correlation”, NASA CR-152241, Lockheed-Georgia Company, Marietta, Georgia, March 1979.

Hess J.L. and Smith A.M.O. (1967), "Calculation of Potential Flow About Arbitrary Bodies", Progress in Aerospace Sciences, Volume 8, Pages 1-138.

Katz J. and Plotkin A. (2001), *Low-Speed Aerodynamics*, 2nd ed., Cambridge University Press.

Mokry M., Chan Y.Y. and Jones D.J. (1983), *Two-Dimensional Wind Tunnel Wall Interference*, Advisory Group for Aerospace Research and Development, North Atlantic Treaty Organization.

Ojha S.K. and Shevare G.R. (1985), “Exact Solution for wind tunnel interference using the panel method”, Computers & Fluids Vol. 13, No.1, pp. 1-14.

Yükselen M. A. (2015), “The role of the configuration aerodynamics in aircraft design and computer support”, FIGES XIX Computer assisted System Modeling Conference, Research and Development in Civil Aviation, and National Aircraft Project, April 21, 2015, Congresium Ankara, (in Turkish).

Yükselen M. A. (2017), Configuration Aerodynamics, Lecture notes, (in Turkish).